

Stabilizing a two-dimensional colloidal solid by light-induced substrates: pinning, depinning and the effect of disorder

This article has been downloaded from IOPscience. Please scroll down to see the full text article.

2008 J. Phys.: Condens. Matter 20 245104

(<http://iopscience.iop.org/0953-8984/20/24/245104>)

View [the table of contents for this issue](#), or go to the [journal homepage](#) for more

Download details:

IP Address: 129.252.86.83

The article was downloaded on 29/05/2010 at 12:40

Please note that [terms and conditions apply](#).

Stabilizing a two-dimensional colloidal solid by light-induced substrates: pinning, depinning and the effect of disorder

D Deb and H H von Grünberg

Karl-Franzens Universität Graz, Institut für Chemie, A-8010 Graz, Austria

E-mail: debabrata.deb@uni-graz.at

Received 23 April 2008

Published 22 May 2008

Online at stacks.iop.org/JPhysCM/20/245104

Abstract

We present Monte Carlo simulations of two-dimensional colloidal solids interacting with disordered and ordered substrate potentials which in practice are created by interfering laser beams. The filling factor η , the number of colloids per potential minimum of the substrate, is taken to be either 1 or $1/9$. For an ordered and commensurate two-dimensional substrate with $\eta = 1$, the solid, being pinned to the periodicity of the substrate, always adopts the perfect order of the substrate, irrespective of the strength of the pinning potential. For $\eta = 1/9$, a solid phase ('floating-solid') with the same translational order decay characteristic as the free solid can form. We explore the nature of this phase and show phase-diagrams containing all three transitions: liquid to pinned-solid, liquid to floating-solid and floating-solid to pinned-solid. We also consider the case of a disordered substrate with a filling factor $\eta = 1/9$ and show that a floating-solid phase can also exist above such a glassy substrate.

(Some figures in this article are in colour only in the electronic version)

1. Introduction

The study of two-dimensional (2D) crystals has a long-standing history in colloid science, beginning with the early work of Pieranski [1]. Nowadays, micrometer colloids located at the air–water interface form almost perfect 2D crystals with grain-boundary-free regions extending over several hundreds of lattice constants and out-of-plane fluctuations of less than 10^{-2} the particle diameter [2, 3]. These systems have been studied with a view towards understanding basic problems in statistical physics, as for example the melting of crystals in two dimensions [3]. More recently, such colloid systems have been taken also as model systems for fundamental problems in the surface sciences. For this, the colloidal systems have been brought into contact with artificial substrates created by interfering laser beams. Several experimental, numerical and theoretical studies of 2D colloids interacting with such light-induced substrates can be found in the literature [4–6].

One of the most intriguing features of 2D solids is the fact that a true long-range crystalline order in two dimensions cannot exist because such a crystal is not stable against thermally excited long-wavelength phonons [7]. On the other

hand, 2D crystals interacting with commensurate substrates are sometimes protected against such an instability. The present paper explores this aspect in more detail; it addresses the question under what circumstances 2D colloidal crystals can be stabilized by means of laser-induced substrates and how they react when exposed to disordered substrates.

To set the stage, we will first consider perfectly commensurate hexagonal substrates with $\eta = 1/9$ and 1 where η is the filling factor giving the ratio between the number of colloids and the number of substrate minima. The effect of periodic light fields on colloidal crystals is to introduce a set of 'springs' connecting each particle to fixed points in space. In [8], it has been shown that for a commensurate light field the additional set of springs will lead to a shift of the phonon bandstructure and that at least two such springs per particle are needed to protect the crystal against the destructive effect of long-wavelength phonons, by lifting the destabilizing jump-singularity of the phonon density of states at the center of the Brillouin zone. Stabilized by such springs, the crystal shows perfect long-range order with a non-decaying translational order parameter. Considering a commensurate hexagonal substrate with $\eta = 1$, there are effectively three springs per

particle connecting each single particle to exactly one site of the hexagonal light lattice. It is clear then that the crystal should always be registered (or ‘pinned’) to the periodicity of the substrate, thus showing the perfect order which the substrate dictates.

Much more interesting therefore is the case when $\eta < 1$, i.e. when the substrate has more minima than there are colloidal particles in the system, because now a competing solid phase (the ‘floating-solid’) can exist [9]. This solid is again not stable: in spite of the presence of a commensurate supportive substrate, the translational order of the floating-solid decays just like that of the free solid. So, for $\eta < 1$ we have the interesting situation that the substrate cannot always stabilize the solid. Whether or not a solid is pinned or floating depends on the colloid–substrate interaction and the temperature. In this paper, we consider two typical colloidal systems and present phase-diagrams showing the melting and depinning transition lines in a plane spanned by temperature and substrate strength. It is mainly this latter variable, the substrate strength, which makes colloidal monolayers on substrates so special, because this strength can be controlled experimentally—in contrast to corresponding surface science systems where the substrate potential cannot be changed.

Given that an ordered substrate can stabilize a 2D solid phase, one is tempted to ask the reverse question as to whether a disordered (glassy) substrate is having a destabilizing effect, i.e. whether a glassy substrate can destroy the order of a 2D solid. This question has already received some attention in the literature, triggered by an early work by Nelson [10] on crystalline films on disordered substrates (with results later corrected in [11]), and continued by more recent studies [12], but has never been brought into context with the peculiar pinned/floating scenario shown by systems with $\eta < 1$. For such systems another interesting question arises; can a floating-solid phase survive when the ordered substrate is replaced by a disordered substrate? This question—explored and discussed again on the basis of the two colloidal systems—will guide us through the second part of the paper.

2. Basic equations and technical details

We here report results for two kinds of colloid–colloid pair-potentials $u(r)$. To represent a system of Yukawa particles, $u(r)$ were chosen to be

$$\beta u(r) = \Gamma \frac{\exp[-2\hat{r}]}{\hat{r}} \quad (1)$$

while an alternative system of superparamagnetic colloids was considered taking

$$\beta u(r) = \frac{\Gamma}{\hat{r}^3} \quad (2)$$

for the interaction potential [3]. Here $\hat{r} = \sqrt{\pi\rho}r$ and Γ are the dimensionless distance and interaction strength, respectively, while $\beta = 1/kT$ is the inverse temperature and ρ the particle area density. In the following, $1/\Gamma$ is alternatively interpreted as the system temperature. Our model Hamiltonian

$$\mathcal{H} = \sum_{i < j} u(r_{ij}) + \sum_i V(\vec{r}_i) \quad (3)$$

consists of two sums, a sum over the colloid–colloid pair-potentials and a sum over the colloid–substrate interactions, where $V(\vec{r}_i)$ is the substrate potential and \vec{r}_i the position of the i th colloid. This Hamiltonian is studied using Monte Carlo (MC) simulations of $N = L^2$ colloidal particles confined to a simulation box of dimensions $L_x = La_0$ and $L_y = La_0\sqrt{3}/2$, where a_0 is the lattice constant of the hexagonal colloidal crystal. The hexagonal substrate is realized in our simulation by using the expression

$$V(x, y) = -v \frac{2}{9} \left(\frac{3}{2} + \cos \frac{4\pi y}{\sqrt{3}a_s} + 2 \cos \frac{2\pi y}{\sqrt{3}a_s} \cos \frac{2\pi x}{a_s} \right) \quad (4)$$

where a_s is the lattice constant of the substrate. Note that $-v \leq V(x, y) \leq 0$ where v is the substrate strength. The lattice constant a_s of the substrate lattice is to be distinguished from the lattice constant a_0 of the colloidal crystal. The ratio of both constants determines what is known as the filling factor $\eta = a_s^2/a_0^2$. Since it counts the number of colloids per substrate minimum, it can also be used when disordered substrates are considered, provided a_s is redefined appropriately. Experimentally, such substrates are realized through the interference pattern of three interfering laser light beams [6].

To study the effect of pinning disorder we have alternatively used a disordered substrate potential, which though having the same number N/η of minima as in the ordered case, have minima positions \vec{R}_i that are randomly distributed over the simulation box of area $L^2 a_0^2 \sqrt{3}/2$. More specifically, we have replaced equation (4) by

$$V(\vec{r}) = \min\{-v \exp(-|\vec{r} - \vec{R}_i|/\xi^2)\}_{i=1, N/\eta} \quad (5)$$

where the range ξ of the individual minimum were chosen such that N/η times $\pi\xi^2$ covers the total area of the simulation box, leading to $\xi^2 = \eta a_0^2 \sqrt{3}/2\pi$. To save computer time we prepared the potential landscape just once before starting the simulation. For this we have divided the whole simulation area into small squares and then set the value of the potential by calculating the substrate potential at the center of the square. Care has been taken to ensure that the sizes of the squares are always much smaller than typical trial MC moves.

Some technical remarks. We have carried out 7×10^6 MC passes through the lattice, 2×10^6 to equilibrate and another 5×10^6 to compute averages. For $L = 60$ (3600 particles), a single data point in figure 2 took about 24 h CPU time on a 2.2 GHz processor. For reasons of numerical efficiency, both pair-potentials were truncated beyond a cut-off radius of $r_c/a_0 = 1.5$. We have also carried out some trial calculations taking a bigger cut-off radius but we did not find any qualitative change in the results. Furthermore, we have employed periodic boundary conditions. As for the random substrate calculations, for each data point the random distribution of \vec{R}_i has been different. Starting from a randomized initial colloidal configurations, the system was again carefully equilibrated which now required much more time than in the ordered case.

As explained in the introduction we need to distinguish a pinned-solid phase from a floating-solid phase. This is achieved by means of the translational order parameter

$$C_{\vec{G}}(\vec{R}_{ij}) = \langle e^{i\vec{G} \cdot [\vec{u}(\vec{R}_i) - \vec{u}(\vec{R}_j)]} \rangle = \langle \cos(G_x u_{xij} + G_y u_{yij}) \rangle \quad (6)$$

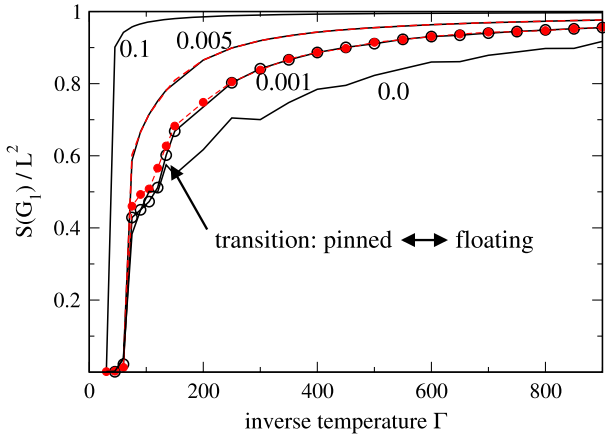


Figure 1. Structure factor at the first-order Bragg peak as a function of the inverse system temperature Γ , for a 2D system of superparamagnetic colloids interacting with a hexagonal substrate, equation (4), of various strengths βv ranging between 0 and 0.1Γ as indicated. The dashed, red lines correspond to a system size of $L = 40$ (1600 particles), the black solid line to $L = 60$ (3600 particles). For $\beta v = 0.001\Gamma$ (lines with circles) a transition floating-solid \leftrightarrow pinned-solid is observed. The free system ($\beta v = 0\Gamma$) melts at $\Gamma_m = 1/T_m = 55$, while the melting point of the system most strongly pinned ($\beta v = 0.1\Gamma$) is shifted to $\Gamma_m = 1/T_m = 30$. Filling factor: $\eta = 1/9$.

where $\vec{u}(\vec{R}) = \vec{r}(\vec{R}) - \vec{R}$ is the displacement of a particle at $\vec{r}(\vec{R})$ from its lattice site \vec{R} while u_{xij}, u_{yij} are the components of $\vec{u}(\vec{R}_i) - \vec{u}(\vec{R}_j)$. G_x and G_y correspond to the components of the reciprocal lattice vector \vec{G} . We here consider reciprocal lattice vectors $\vec{G} = \vec{G}_1$ pointing to a lattice point a distance $4\pi/\sqrt{3}a_0$ away from the center of the first Brillouin zone. While on a regular substrate a pinned-solid shows long-range translational correlations, $C_{\vec{G}_1}(R_{ij}) = \text{const.} > 0$, and a liquid exponentially decaying correlations, $C_{\vec{G}_1}(R_{ij}) \sim e^{-R_{ij}/\xi}$, the correlations of a floating-solid are somewhere in between these two limits, showing an algebraic decay,

$$C_{\vec{G}_1}(R_{ij}) \sim R_{ij}^{-\eta_{G_1}(T)} \quad (7)$$

with the exponent $\eta_{G_1}(T)$ depending on G_1 , the temperature T and the solid's bulk and shear moduli [9]. An alternative way to test for the behavior of the translational correlations is obtained by substituting $C_{\vec{G}_1}(R_{ij})$ for each phase into the structure factor

$$S(\vec{k}) = (1/L^2) \left\langle \left| \sum_j \exp(i\vec{k} \cdot \vec{r}_j) \right|^2 \right\rangle \quad (8)$$

leading to the expression [9, 13]

$$\frac{S(G_1)}{L^2} \sim \begin{cases} 1 & T < T_c & \text{pinned-solid} \\ L^{-\eta_{G_1}(T)} & T_c < T < T_m & \text{floating-solid} \\ (\xi/L)^2 & T_m < T & \text{liquid} \end{cases} \quad (9)$$

which translates each phase's decay characteristic into a typical dependence of the structure factor on the system size L . Here we have introduced two transition temperatures: T_c for the

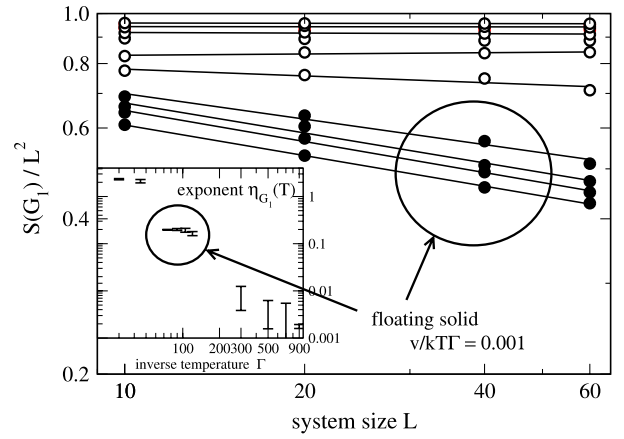


Figure 2. Same quantity as in figure 1, plotted now as a function of the system size L , for $\beta v = 0.001\Gamma$ and for a set of different temperatures. From top to bottom: $\Gamma = 900, 700, 500, 300$ (open circles, L -dependence typical of pinned-solid), $\Gamma = 120, 105, 90, 75$, (filled circles, L -dependence floating-solid). Lines are fits to the expression $L^{-\eta_{G_1}(T)}$ with the resulting exponent $\eta_{G_1}(T)$ shown in the inset. Superparamagnetic colloids.

depinning transition and T_m for the melting transition. Note that the statistics of the calculation of $S(G_1)$ can be improved by averaging over the six \vec{G}_1 s with $G_1 = 4\pi/\sqrt{3}a_0$ which give peaks of structure factors.

When we consider colloidal monolayers interacting with disordered substrates, we compute directly the translational order parameter in equation (6) where now—in addition to the thermal average—an average over different disordered substrate configurations has to be performed. Again, the solid floating over the disordered substrate is characterized by the algebraic decay in equation (7), while now both the pinned and the liquid phase should show an exponential decay of translational order. To determine the phase we fit the simulation data of $C_{\vec{G}_1}(R_{ij})$ to both the function $y(R) = aR^{-b}$ as well as to the function $y(R) = ae^{-bR}$, and then decide what functional form fits better. To this end, we calculate the ratio $\chi_{\text{alg}}^2/\chi_{\text{exp}}^2$ of the goodness-of-fit parameters for fits to the exponential function (χ_{exp}^2) and the algebraic function (χ_{alg}^2). When this ratio is less than 1, this means that the algebraic fit is better while the exponential fit is better otherwise.

3. Results and discussion

3.1. Regular substrate

We first consider perfectly commensurate substrates of the form of equation (4) with a filling factor $\eta = 1/9$. Figure 1 shows how the translational order of the system, as measured by the quantity $S(G_1)/L^2$, behaves as a function of the inverse system temperature Γ for several different values of the substrate strength v . Perfect hexagonal order implies a value of $S(G_1)/L^2$ equal to one, liquid-like order produces values well below 0.1. The plot shows that with increasing v the order of the solid phase generally increases. For $\beta v = 0.1\Gamma$, the system shows a phase transition from the pinned directly into the liquid phase, with a shift of the melting temperature towards higher

temperatures. For $\beta v = 0.001\Gamma$, such a shift is not observed, the behavior is now different. Directly below the melting temperature ($55 < \Gamma < 130$) the order is identical to the order of the free system ($v = 0$), while at even lower temperatures ($\Gamma > 130$) the curves for $\beta v = 0.001\Gamma$ and $\beta v = 0$ differ considerably. The latter phase at temperatures $\Gamma > 130$ is the pinned phase, and is the more ordered one, while the other phase at intermediate temperatures ($55 < \Gamma < 130$) has exactly the same order as the free solid, and thus corresponds to the floating-solid phase. Hence, as expected, the system realizes two distinct solid phases, with a transition point that is somewhere near $T_c = 1/\Gamma_c = 1/130$.

This point can also be estimated from a double logarithmic plot of $S(G_1)/L^2$ versus the system size L , as shown in figure 2. Here the two phases can be easily distinguished by means of equation (9): the pinned-solid should lead to a straight line with zero slope, while the floating phase can be recognized from producing a straight line with finite slope. Fits to the expression $L^{-\eta_{G_1}(T)}$ provide us with values for the exponent $\eta_{G_1}(T)$ which are shown in the inset figure. For lower temperatures ($\Gamma = 900, 700, 500, 300$) the exponent is below 0.01, while for $\Gamma = 120, 105, 90$ and 75 one obtains exponents one order of magnitude larger, consistent with our finding that the depinning transition is near $\Gamma_c = 130$. For $\Gamma = 45$ and 30 , the system is in the liquid phase and the decay of $S(G_1)/L^2$ with L is again an order of magnitude larger, leading to an exponent of around 2 in agreement with equation (9) ($\eta_{G_1}(T) = 2.1 \pm 0.2$ and 2.2 ± 0.2). Exploiting the results of Halperin and Nelson [9], one can calculate the expression $S(G_1)/L^2$ in the limit $T \rightarrow 0$ ($\Gamma \rightarrow \infty$). For the floating phase, one obtains $S(G_1)/L^2 = 1 - c_1 k_B T \ln L$, while for the pinned phase, the result is $S(G_1)/L^2 = 1 - c_2 k_B T/v$, with c_1, c_2 being two irrelevant constants. These expressions confirm that the temperature-driven decay of order slows down proportionally to $1/v$ in the pinned state, but goes logarithmically with system size in the floating state. To explore the order of the depinning transition, we followed the procedure outlined in a similar study on depinning in 2D vortex lattices [14] and calculated histograms of energy density for different system sizes at temperatures near the depinning transition. We were not able to identify two peaks in these histograms, sharpening with increasing system size, as one would have to find for a first-order transition, and thus assume that our depinning transition is a second-order transition.

Figure 3 shows phase-diagrams for both the Yukawa and the superparamagnetic colloids. These diagrams are obtained by determining the transition points from the size-dependence of the structure factor, i.e. from plots such as that in figure 2. We observe that for pinned \rightarrow liquid the shift of the melting temperature is proportional to v and that for the floating \rightarrow liquid the transition is independent of v , which is a direct consequence of the fact that the floating-solid is independent of the substrate. Both diagrams look rather similar, though the radial dependence of the pair-potential is different. The floating-solid phase has also been observed in numerical studies of 2D vortex lattices [13, 14], related XY models [15] and vortex lattices interacting with square pinning arrays [16, 17]. The published phase-diagrams look also

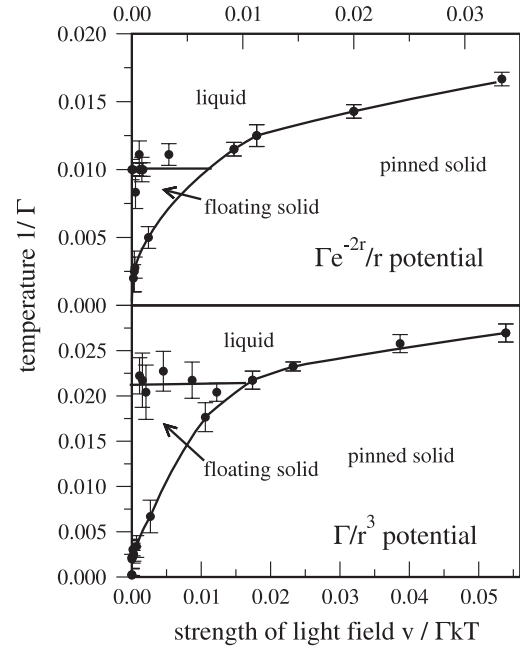


Figure 3. Phase-diagrams spanned by temperature and substrate strength v , for a 2D system of colloids interacting via pair-potentials of the form Γ/\hat{r}^3 (lower panel) and $\Gamma e^{-2\hat{r}}/\hat{r}$ (upper panel).

similar to ours, again for pair-potentials that are completely different from ours. This and the similarity observed in figure 3 allows us to conclude that the details of the pair-potential are not decisive for the appearance of a floating-solid phase. We therefore expect that choosing a longer-ranged cut-off in our pair-potentials would lead to quantitative, but not qualitative changes in the phase-diagram.

One central result of [9] is a criterion quantifying the substrate mesh size below which the floating-solid should be stable to both the pinned and the fluid phase. For our case at hand, this criterion predicts the floating phase to be stable if $\eta < 1/4$, implying that for $\eta = 1$ a floating-solid cannot form. We performed also simulations for a system with $\eta = 1$ (data not shown). No floating phase was found. Instead, the system was always commensurably pinned to the substrate, however small v was chosen, showing always true long-range order and a temperature-dependence of $S(G_1)/L^2$ like that of $\beta v = 0.1\Gamma$ in figure 1, with a direct transition pinned to liquid.

Thus, for $\eta = 1$, not the strength of v , but just the perfectly matching periodicity of the substrate is responsible for the pinning. That is the remarkable stabilizing effect of $\eta = 1$ substrates that has been mentioned in the introduction. On the other hand, for $\eta < 1$ the substrate's capability to pin solely by its periodicity is lost. Now, stabilization requires both a commensurable periodicity and a certain pinning strength. The crystal is pinned only beyond a threshold value of v , see figure 3, and floats out of registry below that value. It then ignores the underlying substrate lattice and behaves as if it were free. On the level of individual particles, the difference between the floating- and the pinned-solid phase can be understood as follows. In the floating-solid phase, individual colloids have enough thermal energy to hop between

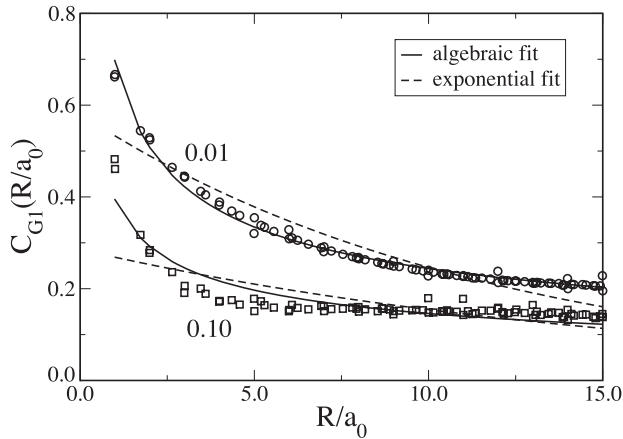


Figure 4. Translational correlation functions, defined in equation (6), as a function of the distance R between lattice sites, for Yukawa particles interacting with a disordered substrate ($\Gamma = 150$). The substrate strength is $v/kT\Gamma = 0.10$ and 0.01 as indicated. The solid and dashed curves are respectively algebraic and exponential fits to the simulation data. System size $L = 60$ ($N = 3600$).

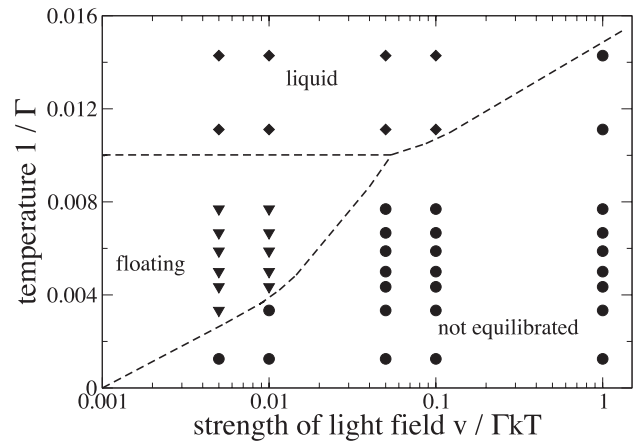


Figure 5. Phase-diagram of a two-dimensional system of Yukawa particles interacting with a disordered substrate. The diagram is spanned by temperature ($1/\Gamma$) and substrate strength v . For parameter combinations of v and Γ indicated by a filled circle, equilibrated results could not be obtained. At all other points, the system is either in the liquid or in the floating-solid phase.

neighboring minima of the light field lattice, with the effect that the mean-square displacement diverges logarithmically as it does for the free crystal. Such a hopping between minima is not possible in the pinned phase, that is, (i) at low temperatures when the colloids do not have enough thermal energy, (ii) at high values of v when the barrier between minima is too high, or (iii) at $\eta = 1$ when free substrate minima are not available in the neighborhood of the particle.

3.2. Random substrate

Having explored the depinning transition of the 2D crystal on the regular substrate, we turn to the disordered substrate, addressing the question as to whether a floating-solid phase is possible also over such a substrate. We consider Yukawa colloids interacting with a disordered substrate of the form given in equation (5); η is taken to be $1/9$, meaning now that there are nine substrate minima per colloid.

At low temperatures and high substrate strengths, the system becomes non-ergodic, so that in a simulation the system cannot find its way to the absolute energy minimum and ends up in a meaningless quenched state somewhere close to the arbitrarily chosen start configuration. This is indicated by the fact that the value of the correlation function $C_{\bar{G}_1}(R)$ for $R \rightarrow \infty$ is non-zero and depends on the initial configuration. In principle, one should have similar problems also in the case of ordered substrates. The difference, however, is that in the presence of an ordered substrate the $T \rightarrow 0$ configuration of the system is known so that one can explore phase space in the neighborhood of this configuration. In contrast, in the case of a disordered substrate the $T \rightarrow 0$ configuration is not known (a priori). Rather, it must be found through simulation, making it necessary to step from higher towards lower temperatures. This is possible only up to a certain temperature beyond which the system unavoidably gets stuck in some local minima. Hence, within the v - T plane, we have some regions that are not accessible because equilibrated results cannot be obtained.

Luckily, the floating solid—which as long as it really floats, is independent of the pinning potential—should not be affected by that problem.

The floating-solid phase can again be clearly identified from its decay behavior. Figure 4 shows the decay characteristic of the system at $\Gamma = 150$ and for $v/kT = 0.01\Gamma$ and $v/kT = 0.10\Gamma$. It is obvious that for $v/kT = 0.01\Gamma$, the simulation data fit much better to an algebraic than to an exponential function ($\chi_{\text{alg}}^2/\chi_{\text{exp}}^2 = 0.6$), indicating that at the point ($\Gamma = 150, v/\Gamma kT = 0.01$) the system is a floating-solid. In contrast, for $v/kT = 0.10\Gamma$, the simulation data fit neither to an algebraic nor to an exponential function; this is caused by the fact that $C_{\bar{G}_1}(R)$ approaches the constant value 0.15 for large distances, indicating that the system is not properly equilibrated at this specific point in parameter space. Analyzing in that way the translational correlation function at several different temperatures and substrate strengths, we finally arrive at the phase-diagram in figure 5, dividing the parameter space into the unaccessible region ($C_{\bar{G}_1}(\infty) \neq 0$) and regions where the correlation functions decay as $y(R) = aR^{-b}$ (floating-solid) or $y(R) = ae^{-bR}$ (liquid phase). In principle, one should be able to find equilibrated results ($C_{\bar{G}_1}(\infty) = 0$) also for the pinned phase where an exponential fit should be better than an algebraic one ($\chi_{\text{alg}}^2/\chi_{\text{exp}}^2 > 1$). However, this was not found. For all points in the solid phase where equilibrated results were obtained, the correlation function decayed algebraically. The resulting phase-diagram is very similar to the corresponding diagram in the upper panel of figure 3, summarizing the results for the ordered substrate. The location of the transition line floating-solid \rightarrow liquid is identical, as it should be. The line corresponding to the depinning transition is at a similar position in both diagrams, though in the absence of a pinned-solid phase this had better not be called a ‘depinning transition’.

Finally, figure 6 shows the temperature-dependence of $S(G_1)/L^2$ for the case of a disordered substrate and compares it to the corresponding curve for the free crystal. This figure

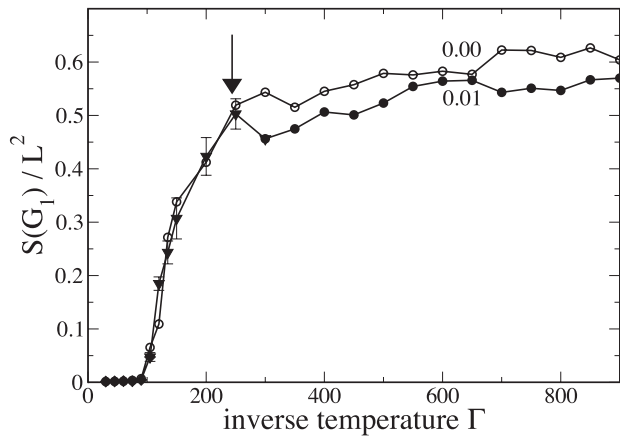


Figure 6. Height of structure factor at the reciprocal lattice site \vec{G}_1 as a function of the inverse system temperature Γ , for a 2D system of N Yukawa colloids interacting with a disordered substrate. The substrate strength is $v/kT\Gamma = 0.01$ and 0.0 (free crystal) as indicated. For $v/kT\Gamma = 0.01$, equilibrated results could be obtained only for $\Gamma < 250$ (triangles with error bars), but not at lower temperatures (filled circles). Error bars result from an average over different realizations of disordered substrates. The melting temperature of the free crystal is $T_m^{-1} = 105\Gamma$. System size $L = 60$ ($N = 3600$).

corresponds to figure 1, showing the same quantity for the regular substrate. Directly below the melting temperature ($105 < \Gamma < 250$, triangles), the order remains identical to the order of the free system ($v = 0$) and becomes different only below a certain lower temperature (marked by an arrow). Below this temperature, we were not able to properly equilibrate the system, the data points in the plot (filled circles) thus correspond to metastable states.

4. Summary and closing remarks

To summarize, we have studied how colloidal solids interact with ordered and disordered substrates. For a commensurate substrate with $\eta = 1$, not the strength, but just the periodicity of the substrate leads to a pinning of the solid to the substrate. The pinned-solid then adopts the perfect order of the substrate, the translational order no longer decays, the mean-square displacement ceases to diverge—the solid is stabilized. For $\eta = 1/9$ the substrate can no longer pin solely by its periodicity. Now, stabilization requires both a commensurate periodicity and a certain pinning strength. Below a threshold value of v , the solid floats out of registry and remains as unstable as the free system. Our phase-diagrams for Yukawa and superparamagnetic colloids in figure 3 show where a floating-solid phase is to be expected within the v - T plane. These diagrams could in principle be measured, for

example with one of the experimental set-ups described in [6]. Particularly interesting would be an experiment which uses a switch between a pinned and a free system to visualize the nature of the 2D instability.

We have also studied the case of a disordered substrate with a filling factor $\eta = 1/9$. We have found that for sufficiently warm crystals and at low pinning strengths the substrate may become too weak to have a pinning effect on the solid, in which case a floating-solid phase can again form, even though the substrate has a glassy order. Thus, a major result of this study is that one can observe a floating-solid phase for a 2D colloid–substrate system for a certain range of substrate strengths irrespective of whether the substrate is regular or irregular. We should finally remark that in a very recent experimental study of colloidal crystals on random pinning potentials [18], it has indeed been verified that the order of the crystal can be destroyed by a random substrate. However, the parameter space (temperature, pinning strength) has not been systematically scanned in search for the existence of a floating-solid phase which we here predict to exist.

Acknowledgments

The authors would like to thank Jörg Baumgartl for his valuable comments. Debabrata Deb received financial support from the Austrian Science Foundation (FWF) under project title P18762.

References

- [1] Pieranski P 1980 *Phys. Rev. Lett.* **45** 569
- [2] Zahn K, Lenke R and Maret G 1999 *Phys. Rev. Lett.* **82** 2721
- [3] von Grünberg H H, Keim P and Maret G 2007 *Soft Matter* vol 3, ed G Gompper and M Schick (Weinheim: Wiley–VCH) chapter 2 pp 41–85
- [4] Brunner M and Bechinger C 2002 *Phys. Rev. Lett.* **88** 248302
- [5] Radzihovsky L, Frey E and Nelson D R 2001 *Phys. Rev. E* **63** 031503
- [6] Bechinger C and Frey E 2007 *Soft Matter* vol 3, ed G Gompper and M Schick (Weinheim: Wiley–VCH) chapter 2, pp 87–158
- [7] Mermin N D 1968 *Phys. Rev.* **176** 250
- [8] von Grünberg H H and Baumgartl J 2007 *Phys. Rev. E* **75** 051406
- [9] Nelson D R and Halperin B I 1979 *Phys. Rev. B* **19** 2457
- [10] Nelson D R 1983 *Phys. Rev. B* **27** 2902
- [11] Cha M C and Fertig H A 1995 *Phys. Rev. Lett.* **74** 4867
- [12] Carpentier D and Le Doussal P 1997 *Phys. Rev. B* **55** 12128
- [13] Franz M and Teitel S 1995 *Phys. Rev. B* **51** 6551
- [14] Gotcheva V and Teitel S 2001 *Phys. Rev. Lett.* **86** 2126
- [15] Hattel S A and Wheatley J M 1995 *Phys. Rev. B* **51** 11951
- [16] Reichhardt C, Olson C J, Scalettar R T and Zimányi G T 2001 *Phys. Rev. B* **64** 144509
- [17] Joseph T and Dasgupta C 2002 *Phys. Rev. B* **66** 212506
- [18] Pertsinidis A and Ling X S 2008 *Phys. Rev. Lett.* **100** 028303